RSC Mechanochemistry

ROYAL SOCIETY OF CHEMISTRY

PAPER

View Article Online
View Journal | View Issue

Cite this: *RSC Mechanochem.*, 2025, **2**, 826

Force governs product diversity in the mechanochemical reactivity of triprismane†

Ankita Das, Chandralekha Hajra and Ayan Datta *

Unlike conventional modes of activation of reactivity, mechanochemical force provides facile and unique pathways. Extensive studies have been performed on the thermal and photochemical interconversions between benzene and its valence isomers. In this article, we show that mechanochemical pulling along 1,2- positions of triprismane (**TP**) can precisely control the outcome, namely, benzene (**BZ**) and/or Dewar benzene (**DB**), depending upon the strength of external force. Within the force range of 1.5–1.9 nN, **DB** is formed exclusively, whereas at forces exceeding ≥2.0 nN, **BZ** becomes the major product. Also, we report that on pulling across 1,4-sites of **TP**, **BZ** is produced exclusively when external force ≥1.8 nN. *Ab initio* steered molecular dynamics (AISMD) simulations on the force modified potential energy surfaces (FMPESs) for 1,2-pulling of **TP** reveal that **DB** becomes the minor product beyond external force ≥2.0 nN. The thermodynamically controlled product, **BZ**, is obtained as the major and sole product for stronger 1,2-pulling and 1,4-pulling respectively. The constrained geometries simulate external force (CoGEF) calculations fail to locate the kinetically trapped intermediate, **DB**, revealing the prowess of AISMD in revealing unique intermediates and fleetingly stable products in the course of mechanochemical reactions. Also, we demonstrate that the **TP** → **BZ** reaction, which demands significant thermal energy, can be induced mechanochemically.

Received 17th April 2025
Accepted 22nd July 2025

DOI: 10.1039/d5mr00050e

rsc.li/RSCMechanochem

Introduction

The concept of a ring structure for benzene was introduced over 150 years ago.[1] About six decades later, Lonsdale employed X-ray diffraction to determine that its six carbon and hydrogen atoms form a regular hexagon.[2] Later, Cox's experimental findings confirmed that benzene is a flat ring molecule.[3] Triprismane was first proposed by Albert Ladenburg in 1869 as a possible structure for benzene though it evaded synthesis until 1973.[4] Other valence isomers of benzene (**BZ**) such as Dewar benzene (**DB**) and Hückel benzvalene were synthesized by Van Tamelen *et al.*[5] and K. E. Wilzbach *et al.* respectively.[6] These isomers, typically referred to as valence-bond isomers of benzene, are obtained *via* photochemical transformation from benzene.[7–10] The distribution of the various valence isomers of benzene is dictated by the medium of reaction,[7–10] nature of the matrix[11] and the wavelength of the irradiated light.[12]

Apart from the experimental progress, several theoretical studies have also gained traction in recent years.[13–16] Dreyer *et al.* computationally demonstrated that the photochemical transformation of benzene into fulvene proceeds *via* a carbene mechanism, involving a prefulvene intermediate.[13] The valence isomers of benzene are photoactive, and therefore, they might switch into other forms under light sources. Isomers such as triprismane and Dewar benzene being highly strained can be excellent candidates for high energy density fuels. Recently, boron–nitrogen containing benzene (azaborine) and its valence isomers[17,18] have been shown to undergo similar photolysis reactions for potential applications in Molecular Solar Thermal (MOST) systems.[19–21] Among all benzene isomers, the parent benzene structure is the most stable, and its unique structure makes it a versatile reagent. While numerous studies have explored how benzene transforms into its valence isomers, its reverse reaction, an exothermic process, remains less explored. Due to significant ring strain, the C–C bonds in triprismane should exhibit high reactivity and undergo transformations with relatively low activation energies. Nevertheless, the highly strained triprismane requires high thermal activation at ~90 °C to transform into benzene (see Scheme 1).[4] Hence, it is quite stable at room temperature.

Mechanophores act as force responsive moieties enabling controlled chemical reactions,[22,23] colour changes,[24] mechanical property modifications[25] or release of small molecules[26] subject to external force or stress. The product diversity is mainly influenced by the site selectivity of the pulling group.[27] Chen *et al.* showed the possibility of isolating different products during the unzipping of a ladderane through the dynamic effects due to bifurcation on the potential energy surface.[28] For a mechanochemical transformation, rupture force (F_{rup}) refers

School of Chemical Science, Indian Association for the Cultivation of Science, 2A and 2B Raja S. C. Mullick Road, Jadavpur, Kolkata, West Bengal, 700032, India. E-mail: spad@iacs.res.in

† Electronic supplementary information (ESI) available. See DOI: https://doi.org/10.1039/d5mr00050e

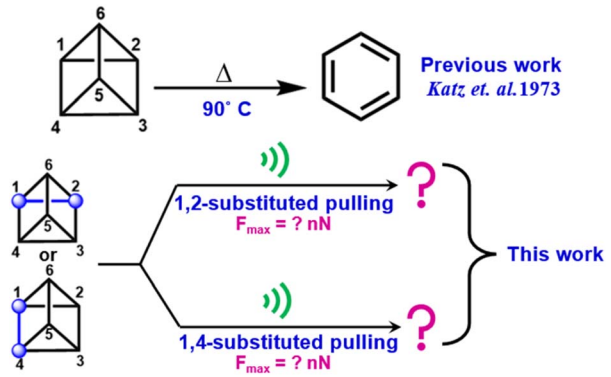

Scheme 1 Isomerization of triprismane under thermal and mechanochemical conditions.

to the minimum external force required for the cleavage of a target bond. It is now established in the expanding domain of mechanochemistry that rupture force can be regulated by altering the strength of the oriented external electric field (OEEF).[29]

Xiaojun *et al.* demonstrated that release of small molecules occurs when sequential application of a mechanical load and photochemical irradiation is performed.[30] Craig and co-workers reported mechanochemical reactivity in the highly strained cubane.[31] Amongst the various pulling positions, only the 1,2-site is mechanochemically successful. Boulatov and coworkers reported that varying the extent of the applied force can lead to different products *via* distinct reaction pathways.[32,33] O'Neill *et al.* illustrated a mechanochemical competition within the same chain between chromophore isomerization and polystyrene backbone cleavage enabling mechanochemical activation under flow in the sonicated solution.[34]

Given the current growing interest in the mechanochemistry of strained ring-systems and the characteristics of triprismane mentioned above, it is a potential candidate for mechanophores. Mechanochemistry of triprismane remains unexplored and we study its potential activation by mechanical force. Pulling at two possible positions namely 1,2- and 1,4- was studied in detail. Although the inexpensive constrained geometries simulate external force (CoGEF) method provides an initial assessment of its mechanochemical pathway, *ab initio* steered molecular dynamics (AISMD) calculations are shown to be important for thermodynamically and kinetically trapped product distribution. The CoGEF calculations fail to predict Dewar benezene (**DB**), and only the thermodynamically controlled product (benzene) is realized. The present article shows that mechanochemical pulling along the 1,2-position of triprismane generates **2,6-DB** at F_{rup} = 1.5–1.9 nN and **1,3-BZ** at $F_{rup} \geq 2.0$ nN.

Computational details

All the constrained geometries simulate external force (CoGEF) calculations and static molecular structure optimizations were performed using the Gaussian 16 suite of quantum chemical programs.[35] The terminal carbon atoms are set as pulling groups where the external force has been exerted upon. The pulling groups are elongated by 0.05 Å at each step until a transformation occurs.[36] The elongation profile of triprismane is obtained from CoGEF calculation at the unrestricted B3LYP/6-31G(d,p)[37] level of theory. Broken symmetry calculations are performed to examine the diradical nature of intermediates in the pathway. From the slope of the inflection point, the rupture force (F_{rup}) is predicted. In all cases, the maximum cut-off for F_{rup} is set to 6.0 nN as beyond this the mechanophore undergoes detachment.[38]

Ab Initio Steered Molecular Dynamics (AISMD) simulations were performed with the TeraChem program suite.[39] The aspects of mechanochemistry of bifurcated pathways have been shown to be accurately captured by AISMD simulations.[28,40,41] The AISMD simulations were carried out using the unrestricted B3LYP functional with the 6-31G basis set.[42] To understand the role of external force in mechanochemical transformation, simulations were executed at various external forces in the range of 1.5 nN to 2.5 nN. All the simulations are performed at a constant external steering force. Terminal carbon atoms were used as the attachment point (AP) and pulled towards 'pulling points' (PPs) defined in 3D space under constant steering force.[43] The pulling points (PPs) were placed about 20 Å away from the AP. All the simulations were done in the canonical (NVT) ensemble using Langevin dynamics at 300 K in the gas phase. The simulations were initiated for 15 ps (picosecond) with a 0.25 fs (femtosecond) timestep and terminated only when a successful chemical transformation was observed. From the AISMD simulations the bond lengths, bond angles and energies were extracted to generate the Force Modified Potential Energy Surfaces (FMPES) under different external forces.[44] The AISMD trajectories are overlaid on the FMPES to understand the reaction pathways leading to products at different external forces.[28]

Results and discussion

To undertake mechanochemical pulling on triprismane, there are two possible pulling sites. A methyl group serves as the pulling group, with the first set at pulling site positions 1 and 2 and the second set at positions 1 and 4. The choice of the pulling group is based on previous theoretical study by Remacle and co-workers.[45] Scheme 2 indicates that upon pulling along the 1,2-positions, a benzvalene intermediate (INT) is formed. In the first step, the cleavage of the C(1)–C(2) bond occurs, followed by bond making between C(1) and C(5) which leads to formation of benzvalene. The rupture force (F_{rup}) was recorded at 3.7 nN from the CoGEF method (see Fig. 1(a)). Formation of INT involves significant diradical character in the pathway (S^2 = 0.9, see Fig. 1(b)). On further pulling, benzvalene gets transferred to the final product benzene *via* simultaneous cleavage of bonds C(1)–C(6) and C(4)–C(5) with rupture force at 4.8 nN. Subsequent to INT formation, the pathway becomes a closed shell.

On the other hand, CoGEF pulling across 1,4-positions gives the same product (**1,4-BZ**) but without producing any intermediate. Mechanochemical pulling produces benzene directly from triprismane by bond breaking of the C(1)–C(4) bond with

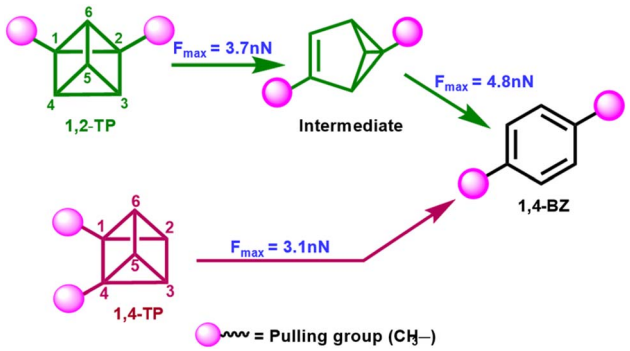

Scheme 2 CoGEF method predicted product formation for 1,2- and 1,4- site pulling along with the rupture forces (F_{rup}).

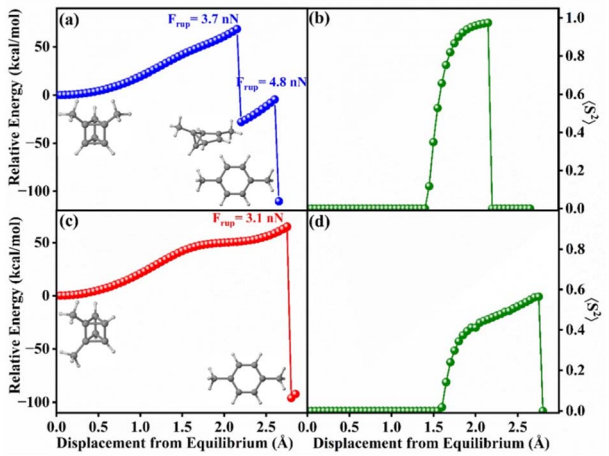

Fig. 1 CoGEF plots at the broken-symmetry UB3LYP/6-31G(d,p) level for (a) pulling across 1,2-positions and (c) pulling across 1,4-positions; the expectation value $\langle S^2 \rangle$ is given in (b) and (d) respectively.

a rupture force (F_{rup}) of 3.1 nN (Fig. 1(c)). This process also involves a diradical pathway ($S^2 = 0.56$, see Fig. 1(d)). Therefore, regardless of the mechanochemical pulling sites, the outcome in both cases is benzene. However, pulling across the 1,4 positions requires less external force for the process.

Since the mechanochemistry of triprismane involves a sequential course of events, the reaction pathway was minutely investigated using *ab initio* steered molecular dynamics (AISMD). The simulations were done under external steering force ranging from 1.5 nN to 2.5 nN for 15 ps. No transformation was observed when pulling occurs with an external force less than 1.5 nN even at longer timescales such as 15 ps. Fig. 2(a) demonstrates that when an external steering force between 1.5–1.9 nN along the 1,2-sites is applied, a mechanochemical transformation toward Dewar benzene (**2,6-DB**) occurs. The process begins with the breaking of the C(1)–C(2) bond, which is then followed by the rupture of the C(3)–C(4) bond, leading to **2,6-DB**. For steering force = 2 nN, about half of the simulation trajectories form benzene (**1,3-BZ**) while the rest form **2,6-DB**, see Table 1. AISMD showed that at first the bond breaking of the C(1)–C(2) bond occurs *via* a diradical pathway and gradually benzene is formed by bond cleavage of C(5)–C(6). In Fig. S1,† $\langle S^2 \rangle$ is plotted over time (in ps) for the simulations performed with forces.

Fig. 2(b) shows the variation in the C(5)–C(6) bond distance with time at different external forces. At least an external force = 2.0 nN is required for **1,3-BZ** formation. At lower external forces, only **2,6-DB** is produced, while intermediate forces yield both **2,6-DB** and **1,3-BZ** as products and higher forces result mainly in **1,3-BZ**. For example, at $F_{steering}$ = 2.5 nN, ~90% of the product is **1,3-BZ**. Unlike the CoGEF calculations discussed in Fig. 1(a) no INT was observed and one additional valence isomer, namely **2,6-DB**, was observed in AISMD simulations.

In contrast, when the pulling occurs along the 1,4 positions with an external force above 1.7 nN, all the simulations result only in **1,4-BZ** as shown in Fig. 2(c). The process involves a diradical pathway by breaking of the C(1)–C(4) bond and then followed by **1,4-BZ** formation (see Fig. S2†). Fig. 2(d) plots the C(1)–C(4) bond distance (Å) with time at various external forces. Unlike the case for the 1,2-pulling, here, the AISMD simulations are in harmony with the CoGEF results. Furthermore, both the CoGEF and AISMD methods indicate that **1,4-BZ** formation is easier for 1,4-pulling.

To analyse the product distribution, the data were extracted from the AISMD calculations and plotted as force-modified potential energy surfaces (FMPESs) to explore the mechanochemical transformation from **1,2-TP** to **2,6-DB** and/or **1,3-BZ** under various applied forces. Fig. 3(a) illustrates the atomic descriptors for the C(1)–C(2) bond and the ∠C(4)–C(1)–C(6) bond angle for forming **1,3-BZ** or **2,6-DB** used in the FMPES plots. In Fig. 3(b)–(e), the generated FMPES at various strains are shown. Fig. 3(b) at F = 0 nN shows all three stationary points, namely, **1,2-TP** (reactant) and two products, **2,6-DB** and **1,3-BZ**. Interestingly, at steering force = 1.5 nN in Fig. 3(c) it is evident that only **2,6-DB** is formed as all the trajectories (red lines) progress towards the **2,6-DB** valley.

However, as the steering force is increased to 2 nN, both **2,6-DB** (red lines) and **1,3-BZ** (blue lines) are formed on the FMPES in Fig. 3(d). It is evident that the deeper potential energy region corresponds to **1,3-BZ** while the shallow one represents **2,6-DB**. The product divergence is well illustrated by the trajectories from AISMD simulations as shown in Fig. 3(d) and (e) at steering forces of 2.0 and 2.5 nN respectively. The FMPES at 2.5 nN in Fig. 3(e) is also indicative of the preferential formation of **1,3-BZ** over **2,6-DB** at higher steering force (*c.f.* **1,3-BZ** : **2,6-DB** = 90 : 10 in Table 1). To observe the change in the FMPES with the increment of external forces the surfaces are plotted in Fig. S3.† The snapshots of the structural change from **1,2-TP** → **1,3-BZ** at 2 nN at different times are illustrated in Fig. 4. For better visualization at 2.0 and 2.5 nN, the FMPESs are presented from multiple angles to clearly illustrate the product distribution in Fig. S5 and S6.† Notably, the **2,6-DB** and **1,3-BZ** wells are not connected by any trajectories. The TS separating two potential wells is ~30 kcal mol^{-1}, making it unlikely that the transformation proceeds through the **2,6-DB** potential well. Note that for 1,4-pulling all the trajectories end up in **1,4-BZ** and, therefore, no other reaction pathways or crossover are observed (see Fig. S7†).

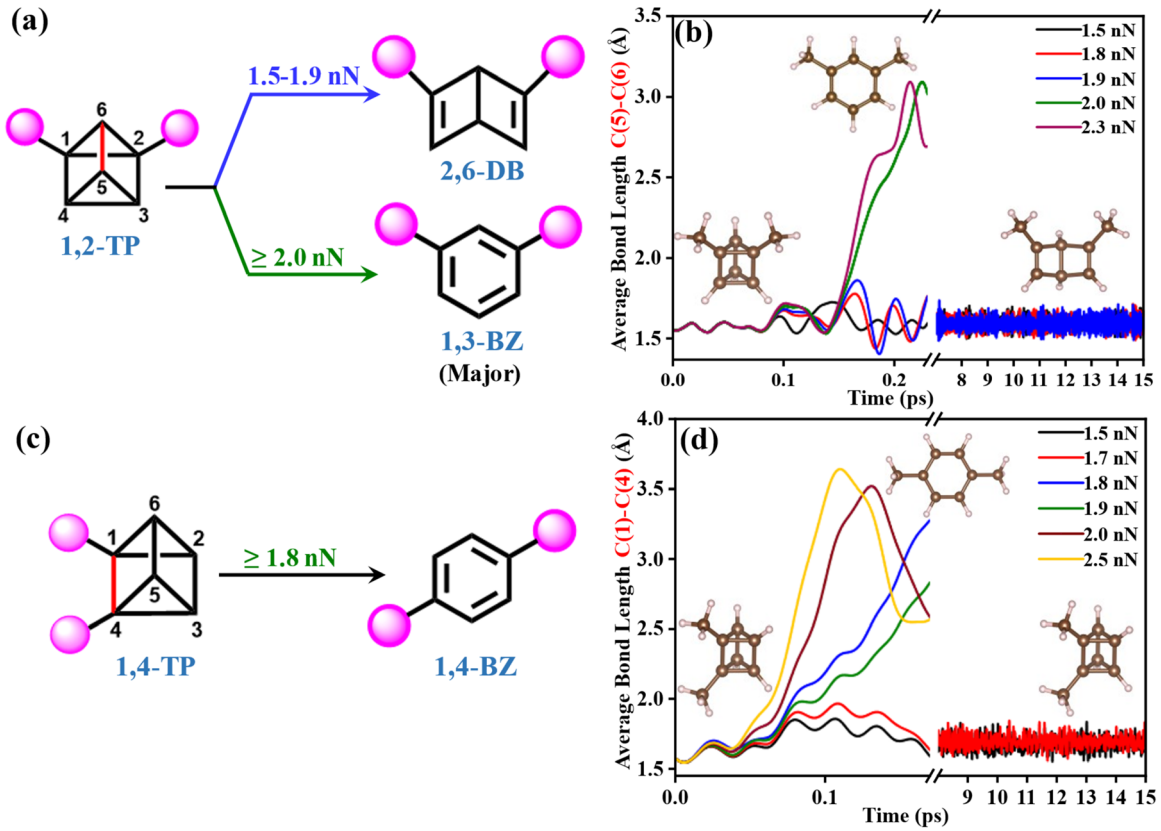

Fig. 2 Product distribution of mechanochemical transformation of triprismane (**TP**) along (a) 1,2-positions at different external forces, (b) AISMD simulations for C(5)–C(6) bond length *vs.* time (ps) for **1,2-TP** → **2,6-DB** and **1,3-BZ** pulling along 1,2-positions, (c) single product formation for pulling along 1,4-positions and (d) AISMD simulations for C(1)–C(4) bond length *vs.* time (ps) for **1,4-TP** → **1,4-BZ** pulling along 1,4-positions.

Table 1 Product distribution qualitative percentage from triprismane to 1,3- & 1,4-benzene and 2,6-Dewar benzene under mechanochemical pulling across 1,2- and 1,4- positions from AISMD

	Pulling along 1,2 positions		Pulling along 1,4 positions	
Steering force (nN)	Yield of **2,6-DB**	Yield of **1,3-BZ**	Yield of **2,6-DB**	Yield of **1,4-BZ**
<1.5	0%	0%	0%	0%
1.5	~100%	~0%	0%	0%
1.8	~100%	~0%	0%	100%
2	~50%	~50%	0%	100%
2.5	~10%	~90%	0%	100%

For an intuitive understanding of the mechanistic trade-off producing 2,6-dimethyl-**DB** and/or 1,4-dimethyl-**BZ** from 1,2-dimethyl-**TP**, the energy profile for the reaction pathway in the absence of external force was computed at the UB3LYP/6-31G(d,p) level. Fig. 5 illustrates that the transformation of 1,2-dimethyl-**TP** into 1,4-dimethyl-**BZ** (along the red pathway) involves two transition states (TS1 and TS2) and the benzvalene intermediate, INT. Formation of INT requires surmounting a massive free-energy barrier ~41.5 kcal mol^{-1} from 1,2-dimethyl-**TP**. Calculations at the DLPNO-CCSD(T)/def2-TZVP//UB3LYP/6-31G(d,p) level also show a large energy barrier = 42.4 kcal mol^{-1} (see Fig. S8†).[40–42] This makes formation of 1,4-dimethyl-**BZ** from 1,2-dimethyl-**TP** kinetically forbidden even though 1,4-dimethyl-**BZ** outstabilizes 2,6-dimethyl-**DB** by 77.7 kcal mol^{-1}. On the other hand, the formation of 2,6-dimethyl-**DB** from 1,2-dimethyl-**TP** as shown in the blue pathway requires a comparatively smaller free-energy barrier of ~28.6 kcal mol^{-1} for TS1′. 2,6-dimethyl-**DB** needs to surmount a free-energy barrier of 29.9 kcal mol^{-1} *via* TS3′ to form 1,3-dimethyl-**BZ**. Therefore, 1,3-dimethyl-**BZ** is the thermodynamically controlled product (TCP) while 2,6-dimethyl-**DB** is the kinetically trapped intermediate.

Interpreting this in the context of the mechanochemistry of 1,2-pulling of **1,2-TP**, at moderate steering forces of 1.5–1.9 nN, the intermediate, namely **2,6-DB**, is formed exclusively. However, when the steering force exceeds 2.0 nN, a TCP namely **1,3-BZ** gets formed preferentially. Given that **1,3-BZ** formation from **1,2-TP** passes through TS1′, TS2′ and TS3′ sequentially, it is possible that at lower external forces, **2,6-DB** is formed as a stable intermediate and does not proceed further. However, at higher forces, **1,3-BZ** is formed.

In contrast, by design, the CoGEF method periodically increases the distance between fixed points on the molecule to estimate the force. In this process the molecule is always under constraint and it might not explore other possible lower energy

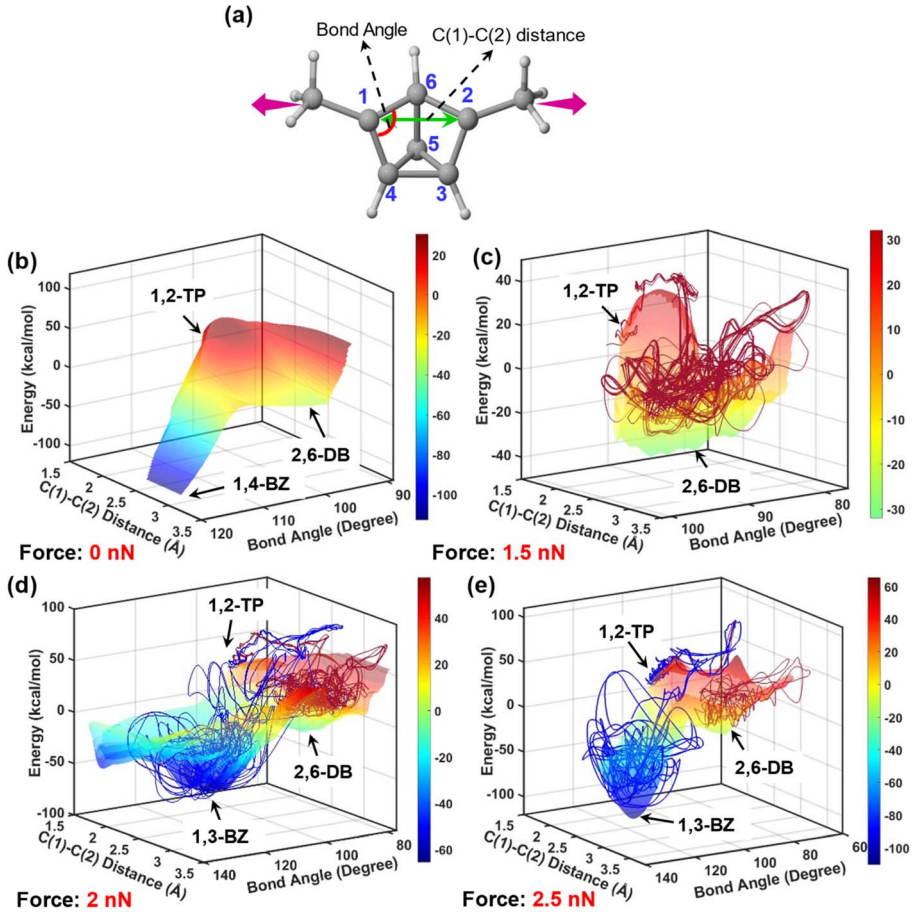

Fig. 3 (a) Schematic representation of pulling along 1,2-positions indicating the bond angle and bond length used in FMPES. FMPESs at (b) 0 nN, (c) 1.5 nN (with the trajectory embedded), (d) 2 nN (with trajectory embedded), and (e) 2.5 nN (with trajectory embedded) showing the significant change in the potential energy surface with increasing external forces. Colour contours: **1,3-BZ** (blue) and **2,6-DB** (yellow–green).

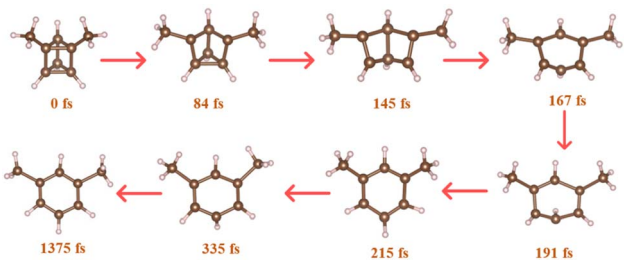

Fig. 4 Representative temporal illustrations for a steering force = 2.0 nN for **1,2-TP** → **1,3-BZ**.

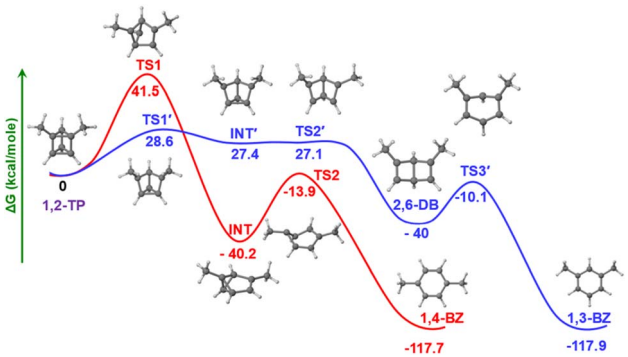

Fig. 5 Free energy profile (at 298 K) for conversion of 1,2-dimethyl substituted triprismane (1,2-dimethyl-**TP**) to 2,6-dimethyl-**DB**, 1,3-dimethyl-**BZ** and 1,4-dimethyl-**BZ** at UB3LYP/6-31G(d,p) in the absence of pulling force.

pathways. Therefore, even though CoGEF offers initial insights into the mechanochemical reactivity yet prediction of the mechanistic pathway for reactions leading to two or more products remains a challenge. In this particular case, CoGEF fails to crossover to a kinetically favourable pathway. This accounts for its failure to locate **2,6-DB** and **1,3-BZ**. AISMD on the other hand allows an exhaustive search for the reaction pathways involving product divergence (*e.g.* geometric configuration/isomers). Nevertheless, even with GPU assistance they are computationally expensive which forces the electronic structure computations only to the modest level (UB3LYP/6-31 G in this case). Therefore, only a limited number of trajectories with various pulling points at each external force can be generated. Hence, a trade-off between the CoGEF and AISMD methods is essential to describe the mechanochemistry of **TP**.

Conclusion

In conclusion, this article illustrates that the strength of the pulling force can induce remarkable diversity in product formation. Not only the position of the pulling groups but also their strength can decide the mechanochemical outcome. The subtleness of mechanochemistry can be richly appreciated in this particular case of **TP** where pulling force <1.5 nN produces no products, **2,6-DB** is produced at pulling force = 1.5–1.9 nN and **1,3-BZ** is produced in majority at pulling force ≥2.0 nN. On the other hand, 1,4-pulling in **TP** exclusively produces **1,4-BZ**. From a wider perspective, the present work also demonstrates the sensitivity of mechanochemical reactions towards experimental reaction conditions such as solvent polarity, sonication frequency and temperature *etc.* as all of these external factors can tune the steering force on the scissile bonds. This is more a boon than a bane as it opens an opportunity to generate seemingly unlikely molecules otherwise.

Data availability

The data supporting this article have been included as part of the ESI.†

Conflicts of interest

There are no conflicts to declare.

Acknowledgements

A. Das thanks DST for the Inspire fellowship. CH thanks CSIR for the senior research fellowship vide 09/0080(18469)/2024-EMR-I. AD thanks SERB (grant no. CRG/2020/000301) for partial funding.

References

1 A. Kekulé, *Bulletin de la Société Chimique de Paris*, 1865, **3**, 98–110.
2 K. Lonsdale, *Proc. R. Soc. London, Ser. A*, 1929, **123**, 494–515.
3 E. G. Cox, *Proc. R. Soc. London, Ser. A*, 1932, **135**, 491–498.
4 T. J. Katz and N. Acton, *J. Am. Chem. Soc.*, 1973, **95**, 2738–2739.
5 E. E. van Tamelen and S. P. Pappas, *J. Am. Chem. Soc.*, 1963, **85**, 3297–3298.
6 K. E. Wilzbach, J. S. Ritscher and L. Kaplan, *J. Am. Chem. Soc.*, 1967, **89**, 1031–1032.
7 L. Kaplan and K. E. Wilzbach, *J. Am. Chem. Soc.*, 1968, **90**, 3291–3292.
8 D. Bryce-Smith, A. Gilbert and D. A. Robinson, *Angew. Chem., Int. Ed. Engl.*, 1971, **10**, 745–746.
9 H. R. Ward, J. S. Wishnok and P. D. Sherman, *J. Am. Chem. Soc.*, 1967, **89**, 162–163.
10 H. R. Ward and J. S. Wishnok, *J. Am. Chem. Soc.*, 1968, **90**, 5353–5535.
11 D. E. Johnstone and J. R. Sodeau, *J. Phys. Chem.*, 1991, **95**, 165–169.
12 D. Bryce-Smith and A. Gilbert, *Tetrahedron*, 1976, **32**, 1309–1326.
13 J. Dreyer and M. Klessinger, *Chemistry*, 1996, **2**, 335–341.
14 I. J. Palmer, I. N. Ragazos, F. Bernardi, M. Olivucci and M. A. Robb, *J. Am. Chem. Soc.*, 1993, **115**, 673–682.
15 M. D. Newton, J. M. Schulman and M. M. Manus, *J. Am. Chem. Soc.*, 1974, **96**, 17–23.
16 U. Deva Priyakumar, T. C. Dinadayalane and G. Narahari Sastry, *New J. Chem.*, 2002, **26**, 347–353.
17 E. M. Arpa, S. Stafström and B. Durbeej, *Phys. Chem. Chem. Phys.*, 2024, **26**, 11295–11305.
18 T. Ozaki and S.-Y. Liu, *Chemistry*, 2024, **30**, e202402544.
19 R. C. Richter, S. M. Biebl, R. Einholz, J. Walz, C. Maichle-Mössmer, M. Ströbele, H. F. Bettinger and I. Fleischer, *Angew Chem. Int. Ed. Engl.*, 2024, **63**, e202405818.
20 T. Ozaki, S. K. Bentley, N. Rybansky, B. Li and S.-Y. Liu, *J. Am. Chem. Soc.*, 2024, **146**, 24748–24753.
21 S. A. Brough, A. N. Lamm, S.-Y. Liu and H. F. Bettinger, *Angew Chem. Int. Ed. Engl.*, 2012, **51**, 10880–10883.
22 S. Mateti, M. Mathesh, Z. Liu, T. Tao, T. Ramireddy, A. M. Glushenkov, W. Yang and Y. I. Chen, *Chem. Commun.*, 2021, **57**, 1080–1092.
23 J. G. Hernández and C. Bolm, *J. Org. Chem.*, 2017, **82**, 4007–4019.
24 M. E. McFadden and M. J. Robb, *J. Am. Chem. Soc.*, 2019, **141**, 11388–11392.
25 S. Akbulatov and R. Boulatov, *ChemPhysChem*, 2017, **18**, 1422–1450.
26 R. Küng, R. Göstl and B. M. Schmidt, *Chemistry*, 2022, **28**, e202103860.
27 A. Das and A. Datta, *J. Am. Chem. Soc.*, 2023, **145**, 13484–13490.
28 Z. Chen, X. Zhu, J. Yang, J. A. M. Mercer, N. Z. Burns, T. J. Martinez and Y. Xia, *Nat. Chem.*, 2020, **12**, 302–309.
29 A. Das and A. Datta, *J. Phys. Chem. B*, 2024, **128**, 6951–6956.
30 X. He, Y. Tian, R. T. O'Neill, Y. Xu, Y. Lin, W. Weng and R. Boulatov, *J. Am. Chem. Soc.*, 2023, **145**, 23214–23226.
31 L. Wang, X. Zheng, T. B. Kouznetsova, T. Yen, T. Ouchi, C. L. Brown and S. L. Craig, *J. Am. Chem. Soc.*, 2022, **144**, 22865–22869.
32 Y. Tian, X. Cao, X. Li, H. Zhang, C.-L. Sun, Y. Xu, W. Weng, W. Zhang and R. Boulatov, *J. Am. Chem. Soc.*, 2020, **142**, 18687–18697.
33 H. Zhang, X. Li, Y. Lin, F. Gao, Z. Tang, P. Su, W. Zhang, Y. Xu, W. Weng and R. Boulatov, *Nat. Commun.*, 2017, **8**, 1147.
34 R. T. O'Neill and R. Boulatov, *Nat. Chem.*, 2023, **15**, 1214–1223.
35 M. J. Frisch, G. W. Trucks, H. B. Schlegel, G. E. Scuseria, M. A. Robb, J. R. Cheeseman, G. Scalmani, V. Barone, G. A. Petersson and H. Nakatsuji, Gaussian Inc., Wallingford CT, 2016, 1, p. 572.
36 I. M. Klein, C. C. Husic, D. P. Kovács, N. J. Choquette and M. J. Robb, *J. Am. Chem. Soc.*, 2020, **142**, 16364–16381.
37 (*a*) P. J. Stephens, F. J. Devlin, C. F. Chabalowski and M. J. Frisch, *J. Phys. Chem.*, 1994, **98**, 11623–11627; (*b*) G. A. Petersson, A. Bennett, T. G. Tensfeldt, M. A. Al-

Laham, W. A. Shirley and J. Mantzaris, *J. Chem. Phys.*, 1988, **89**, 2193–2218.
38 S. M. Luo, R. W. Barber, A. C. Overholts and M. J. Robb, *ACS Polym. Au*, 2023, **3**, 202–208.
39 N. Luehr, A. G. B. Jin and T. J. Martínez, *J. Chem. Theory Comput.*, 2015, **11**, 4536–4544.
40 M. Wollenhaupt, C. Schran, M. Krupička and D. Marx, *ChemPhysChem*, 2018, **19**, 837–847.
41 Y. Liu, S. Holm, J. Meisner, Y. Jia, Q. Wu, T. J. Woods, T. J. Martinez and J. S. Moore, *Science*, 2021, **373**, 208–212.
42 E. C. Garrett and A. Serianni, *Carbohydr. Res.*, 1990, **206**, 183–191.
43 B. D. Mar and H. J. Kulik, *J. Phys. Chem. A*, 2017, **121**, 532–543.
44 M. T. Ong, J. Leiding, H. Tao, A. M. Virshup and T. J. Martínez, *J. Am. Chem. Soc.*, 2009, **131**, 6377–6379.
45 M. Cardosa-Gutierrez, G. De Bo, A.-S. Duwez and F. Remacle, *Chem. Sci.*, 2023, **14**, 1263–1271.